

# Characterization of the Skin Orientation of Thermotropic Liquid-Crystalline Copolyester Moldings with Near-Edge X-Ray Absorption Fine Structure\*

Robert A. Bubeck,<sup>1</sup> Lowell S. Thomas,<sup>1</sup> Stanley Rendon,<sup>2</sup> Wesley R. Burghardt,<sup>2</sup> Alexander Hexemer,<sup>3</sup> Daniel A. Fischer<sup>4</sup>

<sup>1</sup>Michigan Molecular Institute, 1910 W. Saint Andrews, Midland, Michigan 48640-2696

<sup>2</sup>Department of Chemical and Biological Engineering, Northwestern University, Evanston, Illinois 60208

<sup>3</sup>Materials Research Lab, University of California at Santa Barbara, Santa Barbara, California 93106

<sup>4</sup>National Institute of Standards and Technology, Gaithersburg, Maryland 20899

Received 8 November 2004; accepted 21 March 2005

DOI 10.1002/app.22448

Published online in Wiley InterScience (www.interscience.wiley.com).

**ABSTRACT:** The process of injection-molding net-shape parts from thermotropic liquid-crystalline polymers results in a skin-core macrostructure. The underlying orientation in the core and the skin may differ both in magnitude and direction. A combination of near-edge X-ray absorption fine structure (NEXAFS) spectroscopy and two-dimensional wide-angle X-ray scattering (2D WAXS) in transmission was used to characterize the orientation in injection-molded plaques fabricated from thermotropic liquid-crystalline copolyesters based on either 4,4'-dihydroxy- $\alpha$ -methylstilbene or 6-hydroxy-2-naphthoic acid/6-hydroxybenzoic acid. NEXAFS is presented as a noninvasive in situ means of determining surface layer orientation that samples to a

depth of as little as 2 nm and does not require slicing or ultramicrotoming of the samples. The effects of various processing conditions on the surface orientation in the region of the centerline of square injection-molded plaques are presented and discussed. Comparisons are made between orientation parameters obtained by 2D WAXS in transmission, which is dominated by the microstructure in the core, and the NEXAFS technique. © 2005 Wiley Periodicals, Inc. *J Appl Polym Sci* 98: 2473–2480, 2005

**Key words:** injection molding; liquid-crystalline polymers (LCP); orientation

## INTRODUCTION

Thermotropic liquid-crystalline polymers (TLCPs) combine the virtues of superior tensile properties with the ability to injection-mold with very easy flow through the spontaneous ordering of molecules. A critical processing issue is the development of high anisotropy during TLCP processing and its effects on

the physical properties of injection-molded parts. Although the concurrence of high tensile properties and high directional orientation is of great benefit in fiber spinning, severe anisotropy can be a plague in obtaining balanced properties in many injection-molded parts. The rigid nature of the mesogenic segments in TLCP molecules usually leads directly to a high orientational bias favoring the direction of flow with injection molding and other directional processing of thermotropes.<sup>1,2</sup> A skin-core morphology usually develops on the surface and the interior, respectively, of the article during melt processing by extrusion, fiber spinning, injection molding, and so forth.<sup>3</sup>

Layer orientation in injection-molded plaques of 6-hydroxy-2-naphthoic acid (HBA)/6-hydroxybenzoic acid (HNA; 58 mol % HBA and 42 mol % HNA) random copolyesters was determined by Pirnia and Sung<sup>4</sup> with Fourier transform infrared (FTIR) attenuated total reflection dichroism. This technique enabled these researchers to determine the relative orientation encompassing a depth of material 5  $\mu$ m below the sample surface. With measured dichroic ratios to calculate the orientation parameter, the skin, intermediate layers, and core were characterized for a series of samples cut from positions along injection-molded

\*Certain commercial equipment is identified in this article to adequately specify the experimental procedure. In no case does such identification imply recommendation or endorsement by the National Institute of Standards and Technology, nor does it imply that the items identified are necessarily the best available for the purpose.

Correspondence to: R. A. Bubeck (bubeck@mimi.org).

Contract grant sponsor: National Science Foundation; contract grant numbers: DMI-0132519 and DMR-9304725.

Contract grant sponsor: State of Illinois (through the Department of Commerce and the Board of Higher Education); contract grant number: IBHE HECA NWU 96.

Contract grant sponsor: U.S. Department of Energy (Basic Energy Sciences, Office of Energy Research); contract grant number: W-31-102-Eng-38.

Contract grant sponsor: E. I. DuPont de Nemours & Co.

Contract grant sponsor: The Dow Chemical Co.

plaques by the progressive removal of material by milling. Generally, Pirnia and Sung reported the following: (1) orientation was highest for the skin and progressively decreased as one proceeded from the intermediate layers to the core, and (2) orientation was lowest in the gate region of the moldings. The highest orientation was usually observed in the region beyond the immediate gate area, with orientation parameters on the average of 0.77–0.88 being reported for the skin layer. No corroborating techniques were used to verify the FTIR determinations.

Characterizations of TLCPs have also been reported in the literature for the direction of greatest strength in injection-molded tensile bars fabricated from Ticona Vectra HBA/HNA copolyesters by Plummer et al.<sup>5</sup> and Dreher et al.<sup>6</sup> Both research efforts involved examining removed layers and microtomed slices in narrow injection-molded bars by transmission and scanning electron microscopy and by wide-angle X-ray scattering (WAXS). In addition to showing that the tensile modulus increased linearly with the Hermans orientation function, both research groups also indicated that the greatest level of orientation was found in the transition layer between the core and the skin. Molding a plaque or other part with a broad dimensional aspect ratio, however, will incur much greater flow complexity and, therefore, more convoluted orientational states. Shear flow dominates near the surface, whereas transverse stretching dominates near the midplane,<sup>7,8</sup> and this results in a bimodal cross-ply orientation. Depending on the thickness, a skin-core structure also results with a high molecular alignment in the skin that may be maximized in a direction different from that in the core. Shear asserts increasing influence with decreasing sample thickness.

Pirnia and Sung<sup>4</sup> characterized the skin that had encompassed a depth of 5  $\mu\text{m}$  in sampling surface orientation with their FTIR technique. Both Plummer et al.<sup>5</sup> and Dreher et al.<sup>6</sup> were restricted to a distance of about 200–300  $\mu\text{m}$  from the surface of their samples because of the limitations associated with the means of microtoming at their disposal. Because microtoming and slicing are invasive in nature, there is also the possibility of the morphology and orientation being disturbed.

A noninvasive *in situ* means of determining surface orientation offers itself in the form of near-edge X-ray absorption fine structure (NEXAFS). A depth of just 2–3 nm can be selectively characterized with the partial electron yield (PEY) mode of the NEXAFS measurement, and 100 nm can be probed with the fluorescence yield mode. In this study, NEXAFS was validated as a technique for the independent study of surface orientation by the characterization of relatively thin plaques with nearly perfect uniaxial orientation down the centerline of the part. Comparisons were made between the results obtained with NEX-

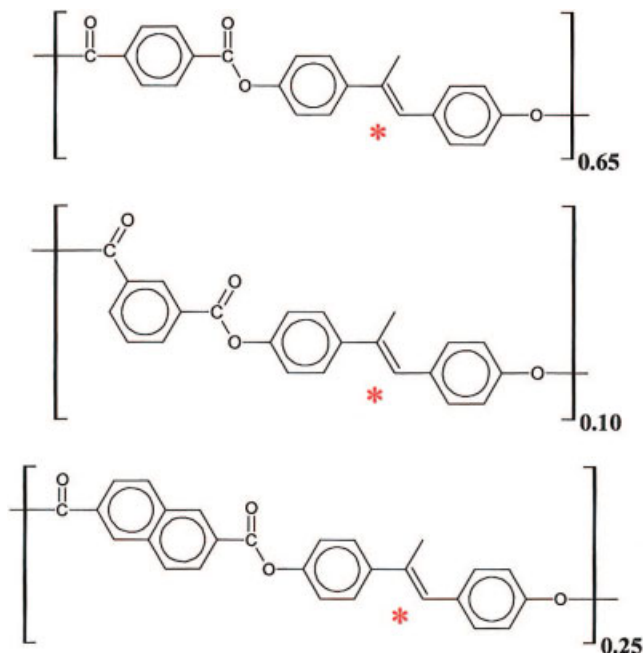


**Figure 1** Chemical structure illustrating the principal components of the DH $\alpha$ MS-based copolyester TLCP. The asterisk denotes the stilbene lineage. [Color figure can be viewed in the online issue, which is available at [www.interscience.wiley.com](http://www.interscience.wiley.com).]

AFS and two-dimensional wide-angle X-ray scattering (2D WAXS) in transmission and, qualitatively, with 2D WAXS results from the literature.

## EXPERIMENTAL

### Materials and fabrication

The TLCP primarily used in this study was a copolyester containing 4,4'-dihydroxy- $\alpha$ -methylstilbene (DH $\alpha$ MS) as the mesogen and a terephthalate/isophthalate/2,6-naphthalenedicarboxylate molar ratio of 65/10/25.<sup>9</sup> The chemical structure for DH $\alpha$ MS is shown in Figure 1. Samples were also molded on a limited basis from Ticona Vectra (Ticona, Florence, KY) A900 containing HBA/HNA copolyesters. Sample plaques (76 mm  $\times$  76 mm) were fabricated with a Boy 30T2 injection-molding machine with which both the melt and mold temperatures were readily controlled. A mold with an insert with polished faces was used, permitting the fabrication of plaques of various thicknesses from 0.8 to 1.6 mm. Polymers with molecular weights of about 35,000 g/mol were evaluated. Fill times of 1 s were used.

It was ascertained that the samples required surface cleaning to remove contaminants before the NEXAFS examination. The cleaning was performed with a 1% solution in deionized water of the Alconox Liqui-Nox cleaning agent (Alconox, White Plains, NY) with a Bransonic 220 ultrasonic cleaner (Bransonic, Danbury,

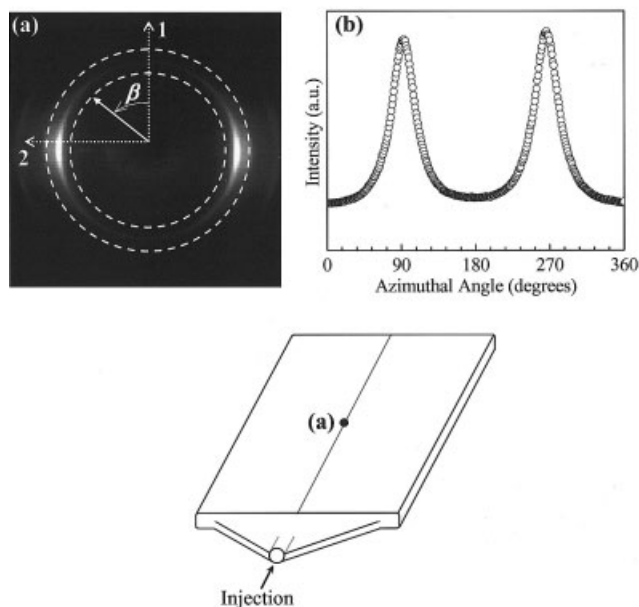


**Figure 2** (a) Physical orientation of an injection-molded plaque along with a representative 2D WAXS pattern taken for a centerline position of a plaque showing a uniaxial contribution to the orientation due to shear flow. The overlays define the coordinates and range of the scattering wave vector used for the extraction of azimuthal scans;  $\beta$  is the azimuthal angle measured away from the vertical filling direction. (b) Representative azimuthal scan obtained from the WAXS pattern.

CT) for 10 min. Both the initial presence of contaminants and their effective removal were verified for selected samples by atomic force microscopy (AFM) with a Topometrix 2000 atomic force microscope.

### X-ray scattering and data analyses of injection-molded plaques

An orientation map for each plaque type was determined by 2D WAXS in transmission performed at 20 keV (0.62 Å) for multiple positions on the samples with the 5BM beam line of the DuPont–Northwestern University–Dow Collaborative Access Team at the Advanced Photon Source of Argonne National Lab. An incident X-ray beam with a 1-mm diameter was used. A Mar CCD detector was used to collect 512 pixel  $\times$  512 pixel raw X-ray scattering patterns with 15 s exposures. 2D WAXS patterns showed significant bimodal contributions from both the core and the skin obtained for 1.6-mm-thick plaques. For the 0.8-mm-thick plaques, uniaxial orientation was dominant along the centerline, and this rendered these samples useful in the comparison of the degree of uniaxial orientation as obtained by 2D WAXS and NEXAFS. Figure 2 provides a representative WAXS pattern at a specific location along the centerline region of a 0.8-mm-thick DH $\alpha$ MS plaque. Details of the data analysis

techniques employed were given by Rendon et al.,<sup>10</sup> however, we present here a more simplified summary.

The program for the 2D WAXS analyses was a MATLAB script that computed the order parameter  $S_S = \frac{1}{2}[3 \cos^2(\phi) - 1]$  (where  $\phi$  is the angle between a given molecule and the principal orientation direction) under the usual Hermans convention.<sup>11</sup> In the limit of perfect orientation, independent of the direction, this quantity will yield a value of 1, whereas 0 reflects a randomized orientation state (i.e., isotropic). In the analysis program, the azimuthally integrated dataset is split into four equal segments whose minimum intensity occurs at zero radians and whose maximum intensity occurs at  $\pi/2$ . The program then computes the order parameters for each of the four regions according to the technique of Mitchell and Windle.<sup>12</sup> This simply involves computing the second Legendre polynomial, which can be correlated to the order parameter. The output gives four values of the uniaxial orientation parameter ( $S$ ) along with the average of the four. Background scattering is accounted for in the computation of the order parameter with a baseline value of the azimuthal intensity (which eliminates any parasitic scattering). This baseline is computed for the WAXS image with the highest anisotropy and corresponding lowest intensity. This value of the intensity is then subtracted from all the other frames in the dataset.

### NEXAFS determinations of surface orientation

The orientation of the skin layer is often difficult to deconvolute from that of the core of a molding when WAXS data obtained in transmission are used. As already cited, Plummer et al.<sup>5</sup> and Dreher et al.<sup>6</sup> did quantify skin orientation in TLCP moldings using WAXS of microtomed layers. A less invasive and laborious means of determining surface orientation directly presents itself, however, in the form of NEXAFS. NEXAFS is a synchrotron-source UV spectroscopy technique that is sensitive to the orientation of phenyl groups via the intensity of the PEY of Auger electrons of the 1s  $\rightarrow \pi^*$  transition of the C=C bonds. The orientation is determined through a series of measurements of the C K edge spectrum over a range of  $\theta$  values of a monochromated linearly polarized UV beam with respect to the sample surface. This technique was successfully used to determine the orientation in liquid-crystalline alignment on rubbed polyimide substrates by Stöhr and Samant.<sup>13</sup> The formalisms behind this technique were refined by Genzer et al.<sup>14</sup> The NEXAFS experiments were performed with the National Institute of Standards and Technology/Dow soft X-ray materials characterization facility (beam line U7A) at the National Synchrotron Light Source at Brookhaven National Laboratory. The capabilities of this beam line have been described elsewhere.<sup>15</sup> The

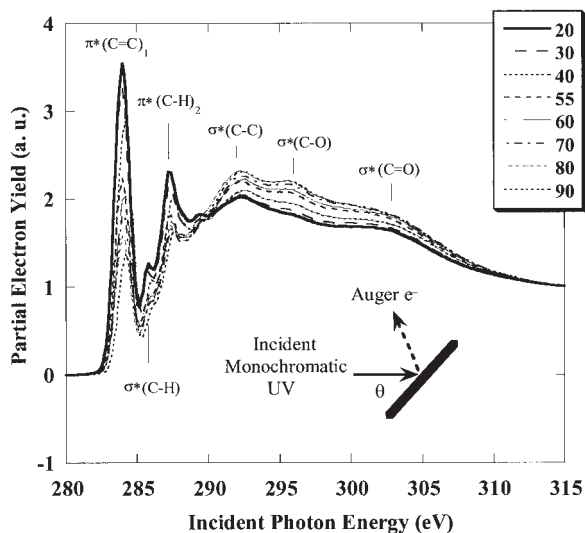


**Figure 3** Sample NEXAFS C K edge spectra for a DH $\alpha$ MS liquid-crystalline copolyester surface. The beam polarization was aligned with the direction of maximum orientation. The process parameters were as follows: melt temperature = 290°C and mold temperature = 45°C.

beam-line soft X-rays had a degree of polarization of about 85% and an incident energy photon resolution and approximate intensity of 0.1 eV and  $5 \times 10^{10}$  photons/s, respectively. The NEXAFS PEY signal was collected with a channeltron electron multiplier fitted with an electrostatic three-grid high-pass electron kinetic energy filter. A grid bias of  $-150$  V was used.

The orientation of the copolyester polymer molecules in the near-surface region (upper 2 nm) was examined with the PEY signals obtained as described previously. Details of the technique as applied to semifluorinated polymers appear elsewhere.<sup>15–17</sup> The PEY spectra for the C K edge were obtained for each sample over the  $\theta$  values with respect to the sample surface of 20, 30, 40, 55, 60, 70, 80, and 90°, normalized in the energy range of 280–315 eV, and the relative intensities,  $I(\theta)$ , for the  $1s \rightarrow \pi^*$  peak for the C=C bonds were recorded. With the technique of Stöhr and Samant,<sup>13</sup> the PEY  $I(\theta)$  value is predicted to take the following form, regardless of the degree of orientation:

$$I(\theta) = A + B\sin^2\theta \quad (1)$$

where  $A$  is the intercept of  $\sin^2\theta = 0$  and  $B$  is the slope or  $I(\theta)$  vs.  $\sin^2\theta$ .  $S$ , parallel to the sample surface, can be calculated as follows:

$$S = -P^{-1}B/[3A + (3 - P^{-1})B] \quad (2)$$

where  $P$  is the beam polarization (0.85 in this case). Values for  $S$  with data obtained over the 30–80°  $\theta$  range were reported to minimize any secondary ef-

facts that could be incurred from surface roughness and/or instrumental anomalies. It was over this more constricted  $\theta$  range that the most linear behavior with the best confidence limits for slope  $B$  was observed. The confidence limit for  $S$  derived from both 2D WAXS and NEXAFS was  $\pm 0.02$ .

### AFM of plaque surfaces

AFM examinations were performed with a Topometrix 2000 in the oscillating mode on the surfaces of a selected number of DH $\alpha$ MS copolyester plaques. Confirmation via AFM of the benefit of ultrasonic surface cleaning of surfaces intended for NEXAFS has already been mentioned in this section.

## RESULTS AND DISCUSSION

An example of a set of NEXAFS C K edge spectra for the surface skin of an injection-molded plaque is shown in Figure 3. The spectra were measured as a function of  $\theta$  of the UV beam with respect to the sample surface. The sample was cut from the middle of the sample close to the vent end edge of a plaque [position 4 in Fig. 6 (shown later)] molded with a melt temperature of 290°C and a mold temperature of 45°C. The  $\pi^*$  (C=C)<sub>1</sub> peaks from the in-plane C=C bonds are minimized when the polarized UV beam is perpendicular to the surface ( $\theta = 90^\circ$ ), and the complementary  $\sigma$ -orbital peaks are correspondingly maximized. This result is consistent with molecular alignment in the plane of the plaque skin and the corresponding  $\pi$  orbital for the C=C bonds being perpendicular to the sample surface. The intensity of the  $\pi^*$  (C=C)<sub>1</sub> peak varies linearly with  $\sin^2$  of  $\theta$ , an

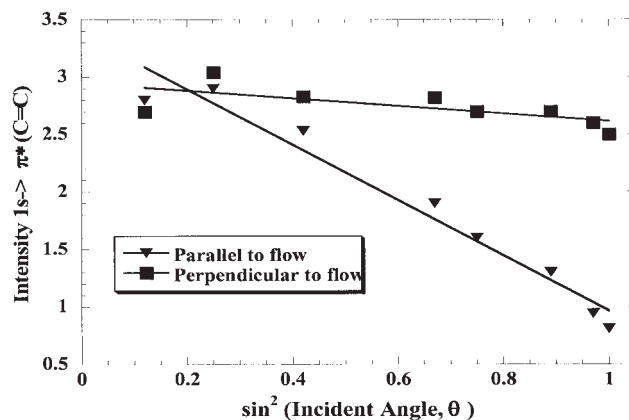


**Figure 4** Example of the angular dependence of the phenyl C=C  $\pi^*$  resonance parallel and perpendicular to the principal direction of shear flow at the surface of an injection-molded DH $\alpha$ MS TLCP plaque. The beam polarization was aligned parallel to the principal flow direction and then perpendicular to the principal flow direction to obtain the two sets of data.

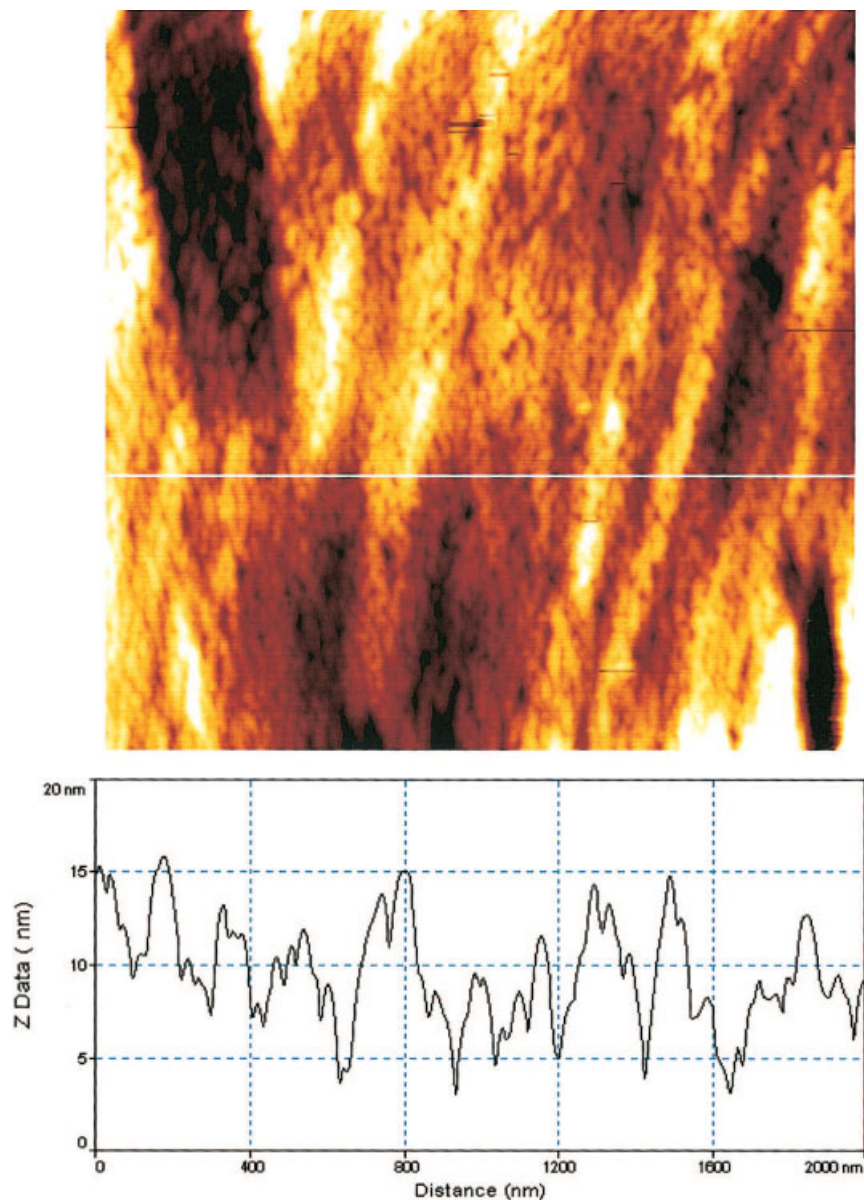


**Figure 5** Sample AFM topology map image of a DH $\alpha$ MS copolyester plaque surface and an accompanying topological profile taken at the indicated horizontal position. The image was obtained 1 cm left of the center of the plaque. The principal flow occurred in approximately the vertical direction. The scales of the ordinate and abscissa are different. [Color figure can be viewed in the online issue, which is available at [www.interscience.wiley.com](http://www.interscience.wiley.com).]

example of which is shown in Figure 4. The determination of the order parameter,  $S$ , was accomplished with eqs. (1) and (2). The nearly flat slope for the case of orientation perpendicular to the flow direction indicates that the surface orientation is almost perfectly uniaxial in the area examined. This general result is identical to that observed by Stöhr and Samant<sup>13</sup> for aligned polyimides and liquid crystals containing phenyl groups in their molecular backbones with cylindrical symmetry about the long axis (i.e., uniaxial nematic) and the  $\pi$  orbitals perpendicular to the long axis. Order parameters derived from the NEXAFS analyses along the centerline of the plaques fabricated

from the studied materials ranged from about 0.25 to 0.65, depending on the position and processing conditions and always with the flow direction in the plane of incidence of the X-ray beam.

Given that NEXAFS is a surface spectroscopy technique, knowledge of the surface topology of the plaques does prove useful. A sample AFM image (topological map) and an accompanying topological surface profile are shown in Figure 5. AFM revealed two principal topological features on the plaque surfaces: a fine texture on the order of 1 nm in height and a much broader feature in the form of corrugations with low gradient slopes on the order of 8 nm in height and 200

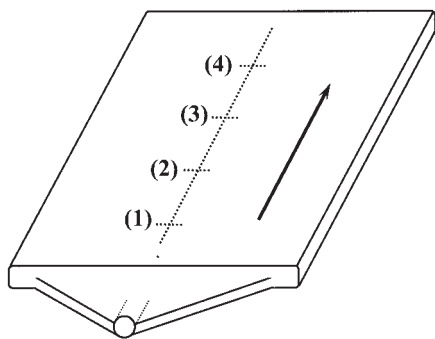


**Figure 6** Injection-molded plaque configuration (76 mm  $\times$  76 mm) with a coat hanger gate shown at the bottom. The arrow indicates the principal flow direction. The numbered positions are 15 mm apart and correspond to those indicated in Figures 7–10. Positions 0 and 5 in Figures 7–10 are the gate-side and exit-side edges of the moldings, respectively.

nm in width at the base. The broad corrugations are aligned in the principal direction of flow. Neither feature was deemed likely to significantly interfere with the NEXAFS measurements.

All NEXAFS data taken and presented in the following discussion were taken with the sample oriented with the flow direction in the plane of incidence. Comparative plots of  $S$  determined at plaque positions 1–4, as defined in Figure 6, are shown in Figure 7(A,B) for two sample molding conditions. The difference between the two conditions is the melt temperature: 245 versus 290°C. For the higher melt temperature, the surface orientation is less than that for the average for the entire sample determined by 2D WAXS in transmission, whereas the average orientation and the orientation at the very surface are nearly identical within the confidence limits of the measurements. This result is also consistent with the observed development of orientation for similar melt temperatures during slit expansion flow by *in situ* WAXS channel flow results reported by Rendon et al.<sup>10</sup> Both Plummer et al.<sup>5</sup> and Dreher et al.<sup>6</sup> also observed that orientation was less on the surface than in the interior (particularly for the transition region between the skin and the core) for HBA/HNA injection moldings fabricated with melt temperatures and mold temperatures in the environs of 280–290 and 80–90°C, respectively. The orientation, as well as the difference in orientation between the skin and the core, is less for the 245°C melt temperature case than for the 290°C case. One can offer the hypothesis that some surface orientation can be lost at a free surface if the polymer is sufficiently above its crystallization temperature. Less orientation is obtained and there is less opportunity for surface relaxation, however, if the melt temperature is relatively close to the crystallization temperature.

As a point of comparison, a NEXAFS-based determination of surface orientation was performed on a

0.8-mm-thick plaque of Vectra A900. The plaque was processed with a 290°C melt temperature and a 45°C mold temperature. Data for a comparison of the surface orientation with the overall orientation determined with transmission WAXS are plotted in Figure 8. The orientation at the very surface is lower than the average orientation throughout the entire thickness obtained by WAXS in transmission. Indeed, this result is similar in kind to the results of both Plummer et al.<sup>5</sup> and Dreher et al.<sup>6</sup> for a similar TLCP processed under fairly similar thermal conditions. The result is also similar to that observed for DH $\alpha$ MS plaques processed at 290°C. Generally, our results agree in kind more closely with those Dreher et al. and Plummer et al. than with those of Pirnia and Sung.<sup>4</sup> Determining whether these differences are related to the process, material, and/or analytical technique would require further investigation.

An example of the effect of the mold temperature on the surface orientation is shown in Figures 9 and 10 for

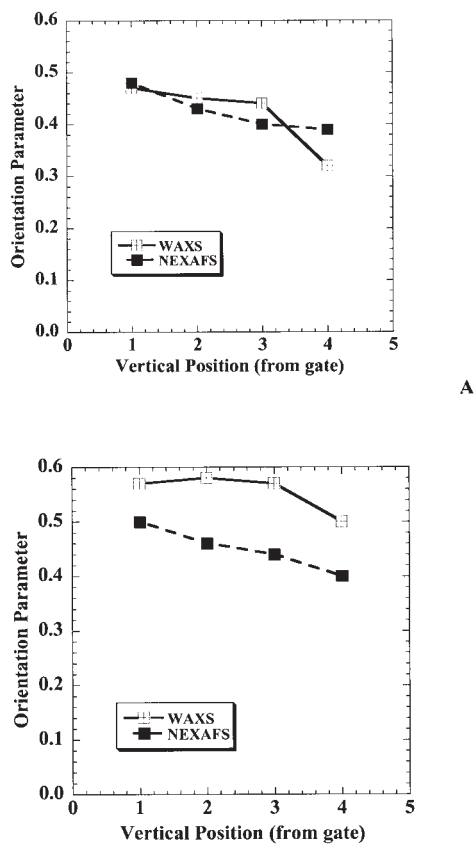


**Figure 7** Comparison of the  $S$  values derived with the NEXAFS method and the WAXS method as a function of the vertical position from the gate in the centerline of two 0.8-mm-thick injection-molded 76 mm  $\times$  76 mm DH $\alpha$ MS plaques: (A) melt temperature = 245°C and mold temperature = 90°C and (B) melt temperature = 290°C and mold temperature = 90°C. The numbered positions correspond to those indicated in

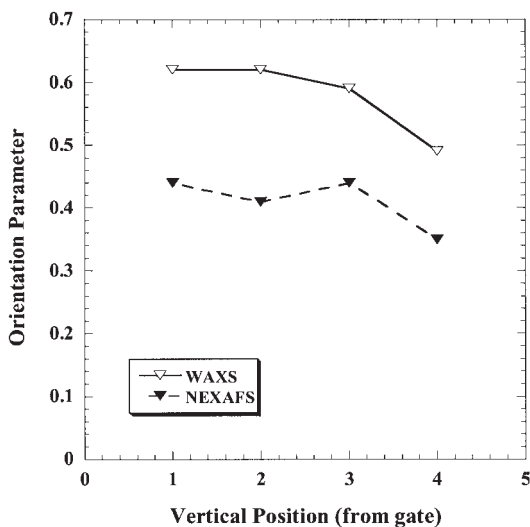


**Figure 8** Comparison of the  $S$  values derived with the NEXAFS method and the WAXS method as a function of the vertical position from the gate in the centerline of two 0.8-mm-thick injection-molded 76 mm  $\times$  76 mm Vectra A900 plaques. The numbered positions correspond to those indicated in Figure 6. The melt temperature was 290°C, and the mold temperature was 45°C. The samples were processed under nearly pure shear flow conditions with little contribution from transverse flow.

two melt temperatures. At a melt temperature of 290°,  $S$  ranges from about 10 to 20% more for a 45°C mold temperature than for a 90°C mold temperature; this result is consistent with what one might expect as a result of more rapid cooling and crystallization derived from the colder mold. If a more unusual melt

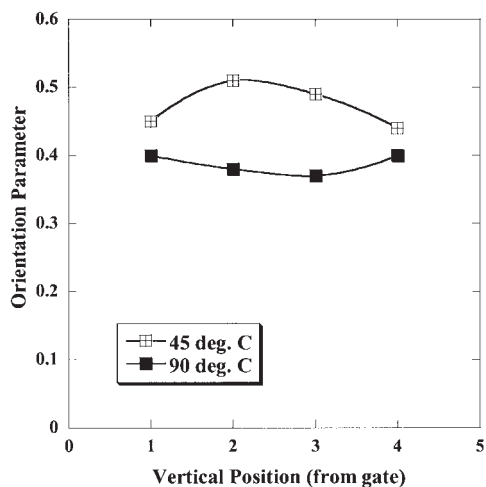


**Figure 9** Comparison of the  $S$  values for two mold temperatures derived with the NEXAFS method as a function of the vertical position from the gate in the centerline of two 1.6-mm-thick injection-molded 76 mm  $\times$  76 mm DH $\alpha$ MS plaques. The numbered positions correspond to those indicated in Figure 6. The melt temperature was 290°C, and the mold temperatures were 45 and 90°C.

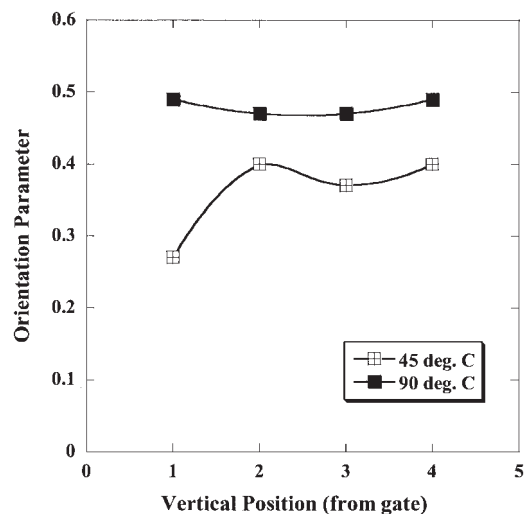


**Figure 10** Comparison of the  $S$  values for two mold temperatures derived with the NEXAFS method as a function of the vertical position from the gate in the centerline of two 1.6-mm-thick injection-molded 76 mm  $\times$  76 mm DH $\alpha$ MS plaques. The numbered positions correspond to those indicated in Figure 6. The melt temperature was 245°C, and the mold temperatures were 45 and 90°C.

temperature of 245°C is chosen at the low end of the melting transition, then the relative orientations obtained for the same two mold temperatures reverse their ranking for retained surface orientation. The higher mold temperature is required to obtain a relatively uniform orientation for the four plaque positions, particularly on the gated end (position 1).

Comparisons of the surface orientation are presented and discussed in this article. The positions off the centerline are the areas governed by more complex flow conditions. Future work will entail characterizations of the state of orientation with a six-axis sample manipulator for positions distanced from the centerline. The ability to rotate the sample azimuthally will enable the accurate determination of the surface orientation in the regions of greater complexity. The NEXAFS technique has the additional capability of determining the magnitude of the biaxial nematic character, as described by Donald and Windle,<sup>1</sup> if it exists (see ref. 12). Future work shall include measurements away from the centerline of the plaques with azimuthal and  $\theta$  measurements to determine if nematic biaxiality is required to fully describe the orientation state for skin layers of TLCPs.

## CONCLUSIONS

The contributions of shear and extensional flows to the bimodal orientational character of the moldings have been characterized by a combination of NEXAFS spectroscopy and 2D WAXS in transmission. NEXAFS and 2D WAXS have been used to characterize the orienta-

tion in injection-molded plaques fabricated from thermotropic liquid-crystalline copolyesters based on either DH $\alpha$ MS or HBA/HNA. NEXAFS has been presented as a noninvasive *in situ* means of determining surface layer orientation that samples to a depth as shallow as 2 nm and does not require slicing or ultramicrotoming of the samples. The equivalency of orientation parameters obtained with 2D WAXS in transmission and NEXAFS techniques has been verified with a selected pure shear flow processing set of conditions for a thin 0.8-mm-thick plaque for which little relaxation time before crystallization was permitted. The surface orientation parameters range from 0.27 to 0.65 for the materials and processing conditions studied. The orientation of the surface layer of the skin of the moldings examined is less than that for the average through-thickness orientation, as determined by 2D WAXS in transmission, except for a melt processing temperature at the low end of the melting transition.

The near-edge X-ray absorption fine structure experiments were carried out at the National Institute of Standards and Technology/Dow soft X-ray materials characterization facility at the National Synchrotron Light Source of Brookhaven National Laboratory, which is supported by the U.S. Department of Energy Division of Materials Sciences and Chemical Sciences. Wide-angle X-ray scattering experiments were conducted at the DuPont-Northwestern-Dow Collaborative Access Team (DND-CAT) Synchrotron Research Center located at Sector 5 of the Advanced Photon Source of Argonne National Laboratory. DND-CAT is supported by E. I. DuPont de Nemours & Co., Dow Chemical Co., the National Science Foundation, and the State of Illinois through the Department of Commerce and the Board of Higher Education. Use of the Advanced Photon Source was supported by the U.S. Department of Energy (Basic Energy Sciences, Office of Energy Research). The authors thank Edward J. Kramer (University of California at Santa Barbara), Xuefa Li

(Cornell University), and Christopher K. Ober (Cornell University) for their collaboration during the various stages of this project. The assistance of Mathew Stephenson (Michigan Molecular Institute) in obtaining the atomic force microscopy data is greatly appreciated.

## References

1. Donald, A. M.; Windle, A. H. *Liquid Crystalline Polymers*; Cambridge University Press: Cambridge, England, 1992.
2. Onogi, S.; Asada, T. In *Rheology*; Astarita, G.; Marrucci, G.; Nicolais, L., Eds.; Plenum: New York, 1980; Vol. 1.
3. Sawyer, L. C.; Jaffe, M. *J Mater Sci* 1986, 21, 1897.
4. Pirnia, A.; Sung, C. S. P. *Macromolecules* 1988, 21, 2699.
5. Plummer, C. J. G.; Zulle, B.; Demarmels, A.; Kausch, H.-H. *J Appl Polym Sci* 1993, 48, 751.
6. Dreher, S.; Seifert, S.; Zachman, H. G.; Moszner, N.; Mercoli, P.; Zanghellini, G. *J Appl Polym Sci* 1998, 67, 531.
7. Cinader, D. K.; Burghardt, W. R. *J Polym Sci Part B: Polym Phys* 1999, 37, 3411.
8. Bubeck, R. A.; Thomas, L. S.; Burghardt, W. R.; Rendon, S.; Hexemer, A.; Hart, B. *Churchill Conf Deformation Yield Fract Polym* 2003, 12, 155.
9. Bales, S. E.; Hefner, R. E.; Singh, R. (to Dow Chemical Co.). U.S. Pat. 5,614,599 (1997).
10. Rendon, S.; Burghardt, W. R.; New, A., II; Bubeck, R. A.; Thomas, L. S. *Polymer* 2004, 45, 5341.
11. Hermans, P. H.; Platzek, P. *Kolloid Z* 1939, 88, 68.
12. Mitchell, G. R.; Windle, A. H. In *Developments in Crystalline Polymers 2*; Basset, D. C., Ed.; Elsevier: London, 1988.
13. Stöhr, J.; Samant, M. G. *J Electron Spectrosc Relat Phenom* 1999, 98, 189.
14. Genzer, J.; Kramer, E. J.; Fischer, D. A. *J Appl Phys* 2002, 92, 7070.
15. Genzer, J.; Sivaniah, E.; Kramer, E. J.; Wang, J.; Xiang, M.; Korner, H.; Char, K.; Ober, C. K.; DeKoven, B. M.; Bubeck, R. A.; Chaudhury, M. K.; Sambasivan, S.; Fischer, D. A. *Macromolecules* 2000, 33, 1882.
16. Genzer, J.; Sivaniah, E.; Kramer, E. J.; Wang, J.; Xiang, M.; Char, K.; Ober, C. K.; Bubeck, R. A.; Fischer, D. A.; Graupe, M.; Colorado, R.; Shmakova, O. E.; Lee, T. R. *Macromolecules* 2000, 33, 6068.
17. Genzer, J.; Sivaniah, E.; Kramer, E. J.; Wang, J.; Xiang, M.; Korner, H. M.; Char, K.; Ober, C. K.; DeKoven, B. M.; Bubeck, R. A.; Fischer, D. A.; Sambasivan, S. *Langmuir* 2000, 16, 1993.